Monitoring the coastal zone using earth observation:

Ettritch, Georgina; Bunting, Peter; Jones, Gwawr Angharad; Hardy, Andrew

Published in:
Remote Sensing in Ecology and Conservation

DOI:
10.1002/rse2.79

Publication date:
2018

Citation for published version (APA):
Ettritch, G., Bunting, P., Jones, G. A., & Hardy, A. (2018). Monitoring the coastal zone using earth observation: application of linear spectral umixing to coastal dune systems in Wales. *Remote Sensing in Ecology and Conservation*, *4*(4), 303-319. https://doi.org/10.1002/rse2.79

Remote Sensing in Ecology and Conservation
Open Access
ZSL LET'S WORK FOR WILDLIFE

ORIGINAL RESEARCH

Monitoring the coastal zone using earth observation: application of linear spectral unmixing to coastal dune systems in Wales

Georgina Ettritch[1], Peter Bunting[1], Gwawr Jones[2] & Andy Hardy[1]

[1]Department of Geography and Earth Sciences, Aberystwyth University, Aberystwyth SY23 3DB, United Kingdom
[2]JNCC, Monkstone House, City Road, Peterborough, Cambridgeshire PE1 1JY, United Kingdom

Keywords
Ecosystem monitoring, Landsat, linear spectral unmixing, multispectral, sand dunes, WorldView2

Correspondence
Georgina Ettritch, Department of Geography and Earth Sciences, Aberystwyth University, Aberystwyth SY23 3DB, United Kingdom.
Tel: +44 (0)1970 628 552; Fax: +44 (0)1970 622 659; E-mail: gge9@aber.ac.uk

Funding Information
Georgina Ettritch's, MSc was funded by the European Social Fund (ESF) through the European Union's Convergence programme administered by the Welsh Government, with the support of Environment Systems Ltd as the industrial partner.

Editor: Harini Nagendra
Associate Editor: Kate He

Received: 23 September 2017; Revised: 13 February 2018; Accepted: 22 February 2018

doi: 10.1002/rse2.79

Abstract

Coastal sand dune systems across temperate Europe are presently characterized by a high level of ecological stabilization and a subsequent loss of biological diversity. The use of continuous monitoring within these systems is vital to the preservation of species richness, particularly with regard to the persistence of early stage pioneer species dependent on a strong sediment supply. Linear spectral unmixing was applied to archived Landsat data (1975–2014) and historical aerial photography (1941–1962) for monitoring bare sand (BS) cover dynamics as a proxy for ecological dune stabilization. Using this approach, a time series of change was calculated for Kenfig Burrows, a 6-km^2 stabilized dune system in South Wales, during 1941–2014. The time series indicated that a rapid level of stabilization had occurred within the study area over a period of 75 years. Accuracy assessment of the data indicated the suitability of medium-resolution imagery with an RMSE of <10% across all images and a difference of <3% between observed and predicted BS area. Temporal resolution was found to be a significant factor in the representation of BS cover with fluctuations occurring on a sub-decadal scale, outside of the margin of error introduced through the use of medium-resolution Landsat imagery. This study demonstrates a tractable approach for mapping and monitoring ecologically sensitive regions at a sub-Landsat pixel level.

Introduction

On a global scale, coastal dune systems are experiencing heightened levels of ecological stabilization predominantly induced by global warming and associated climate change (Provoost et al. 2011). Reduction in storm magnitude frequency, for example, causes the reduction in offshore sediment supply necessary for the colonization of pioneer species (Tsoar 2005; Pye and Blott 2011). Associated rise in sea level also increases the risk of erosion at the dune toe and has been found to induce phases of net sediment loss from the system (Saye and Pye 2007). Stabilization is further enhanced by increases in nitrogen concentrations from atmospheric and groundwater sources, exacerbating plant productivity and growth (Jones et al. 2002, 2004). The direct effect of stabilization under such conditions is a reduction in ecological biodiversity whereby the number of sand-dependant pioneer species is depleted as mature stands become established under a low sediment supply regime (Tsoar and Møller 1986; Karnieli 1997; Levin and Ben-Dor 2004).

The coastline of Wales, UK is a prime example of a temperate region where coastal dune systems predominantly exist under an ecologically stabilized regime. Stabilization within this region is not only the result of contemporary climatic conditions, but is also a product of human intervention between the 14th and late 20th century (Hoffman et al. 2005; Pye et al. 2007; Clarke and Rendell 2009, 2011; Plassmann et al. 2010; Pye and Blott 2012). Over 55% of dune systems in Wales are currently subject to a net loss of sediment (Dargie 1995). Current attempts at mitigation are precariously positioned in relation to long-term climate variations. Despite sub-decadal variations, the last two centuries have experienced negligible long-term change in storm magnitude frequency within northern Europe (Clarke and Rendell 2011). Therefore, potential management strategies aimed at stabilization reduction implemented under this stable climatic regime may have untold consequences in the future under changing conditions. For this reason, it is vital that these ecosystems are continuously monitored to inform future adaptive management of the coastal zone, particularly with regard to the propagation and preservation of pioneer species. So far, biodiversity monitoring strategies have favoured the use of discrete traditional field-based techniques (e.g. quadrat-based species composition) that are labour intensive thereby reducing spatial coverage and repeatability.

Remote sensing technologies can be used to monitor land cover conditions at scales suitable for coastal habitat management. Previous attempts have made use of high-spatial resolution datasets including Compact Airborne Spectral Imager (CASI) hyperspectral imagery (Shanmugam and Barnsley 1998; Lucas et al. 2002; Shanmugam et al. 2003; Thackrah et al. 2004; Pye and Blott 2012; Zhang and Baas 2012). However, due to the cost and coverage of aerial surveillance campaigns, these sources of data are unlikely to provide an operationally viable technique for high frequency monitoring. Freely available satellite data sources such as the Landsat mission offer a rich archive of historical imagery (from 1972) and ensure mission continuity into the future.

Previous studies have already demonstrated the importance of semi-automated monitoring in aeolian environments to inform adaptive management using Landsat data, at the dune system to sand sea scale. For example, change detection was implemented in Western Australia to determine the influence of fire on sand dune reactivation from 1988 to 2016 (Shumack et al. 2017). Multitemporal analysis of burn scar area and sand abundance determined that while fire increased potential vulnerability to dune destabilization within the study region, it was not the primary driver (Shumack et al. 2017). Medium-resolution optical data are also useful in the monitoring of active dune systems where the primary threat is sand encroachment on peripheral land use, rather than the loss of biodiversity. For example, archived Landsat imagery (1992–2010) was used to map the direction and distance of annual dune migration within two dune systems in California. The aim was to assess the risk of sand encroachment on renewable energy installations proximal to active dunes (Potter and Weigand 2016). Furthermore, similar studies using Landsat have been conducted across agricultural regions threatened by large-scale desertification from climate change and human activity such as in the Sahel (Ahmady-Birgani et al. 2017; Salih et al. 2017; Zhang et al. 2018).

However, while useful medium-resolution data (30–60 m) is often associated with pixels that include multiple spectrally distinct land cover types. These mixed pixels can result in the loss of key indicators of ecological diversity and dune stability when semi-automated classification techniques at pixel level are used. Accordingly, image analysis techniques aimed at unmixing land cover fractions at the subpixel level offer a viable approach for the assessment of ecological stabilization within sand dune systems. The subsequent aim of this study was to assess the potential for monitoring ecological stabilization levels using linear spectral unmixing (LSU), as a subpixel image analysis technique. The study focused on the subpixel detection of bare sand (BS) cover as a proxy for ecological stabilization over time in Landsat satellite imagery and historic aerial photography.

Linear spectral unmixing

Theoretical foundations

The process of LSU is derived from the linear mixture model (LMM). The LMM was initially developed by (Horwitz et al. 1971) and assumes that the reflectance of a pixel is a linear combination of the reflectance of all subpixel components (known as endmembers), weighted by abundance (Adams et al. 1995). The integrity of the model is therefore dependent on the assumption that photons only have a single interaction with a surface represented by a pixel (Adams et al. 1993). A more detailed description of the LSU process can be found in (Adams et al. 1993; Sohn and McCoy 1997; Drake et al. 1999; Gong and Zhang 1999; Weng et al. 2004; Barducci and Mecocci 2005; Somers et al. 2009; Silván-Cárdenas and Wang 2010; Van der Meer and Jia 2012).

The LSU model is subject to two constraints in order to successfully honour the fundamental assumption of spectral linearity. First, endmember fractions must sum to unity, that is, the abundance of all components within a pixel must sum to 1 (representing spatial continuity of

the landscape). Second, all abundance estimates must be ≥0 as a component can only ever be existentially present or absent from a pixel (Rajabi and Ghassemian 2013). This can be expressed mathematically where fi is the abundance of the k^{th} endmember within the i^{th} pixel and p is the total number of endmembers.

$$\sum_{k=1}^{p} fik = 1 \qquad fik \geq 0 \tag{1}$$

Non-negative constraints are notoriously difficult to fit to the LSU model during implementation (Heinz and Chang 2001), and subsequently, popular software packages (e.g. ENVI) exclude this constraint (Silván-Cárdenas and Wang 2010). Overall, there is a general preference within present research for partially constrained models, which only sum to unity. Within partially constrained applications, a mitigative correction is often applied post-unmixing which rectifies numerical negativity. As such, negative fractions are given a value of 0 and the remaining fractions >0 are normalized to reflect unity (Zhang and Baas 2012). However, this post-unmixing technique does not optimize abundance estimation accuracy as the constraints are applied sequentially rather than simultaneously (Heinz and Chang 2001). Subsequently, there has been a proliferation of research aimed at the development of fully constrained approaches (Chang and Heinz 2000). However, these new techniques have been criticized for their computational complexity in comparison to partial constraining, rendering them unsuitable for application to large-scale datasets (Hu et al. 1999).

Endmember selection

Residual error within an LSU model originates from endmember identification. A key point of origin is connected to the extraction of spectral endmembers from the image data cloud, particularly in relation to the introduction of human error. For example, (semi-)automated endmember extraction algorithms, such as the Pixel Purity Index (PPI) (Chang 2013), are aimed at isolating and selecting purest spectral pixels from a dataset. However, they are limited by the potential for human error introduced through arbitrary parameter selection during implementation (Chang and Plaza 2006).

Furthermore, it is an assumption of traditional spectral mixture analysis that a single, pure endmember signature can be an exact, invariable representation of its reciprocal component. However, in practice, image components are capable of experiencing multiple degrees of intraclass variability, and subsequent interclass separability (Wang and Jia 2009). Within an ecological context, this can be attributable to plant phenology (Song 2005) and species-based biochemical properties (Smith et al. 1994; Asner 1998; Ustin et al. 1999; Asner and Lobell 2000; Serrano et al. 2002). For example, at the biochemical level, spectral variability has been attributed to the concentration of nitrogen and foliar lignin, relating to maximum photosynthetic and litter decomposition rates respectively (Serrano et al. 2002).

Over the last three decades, numerous LSU techniques have been developed to account for spectral variance within endmembers. Due to its computational simplicity, spectral averaging has traditionally been a popular technique (Kerdiles and Grondona 1995; Small 2012). Averaging incorporates variability by producing one representative signature from a library of potential variations. However, this approach is based on the assumption that spectral variations of an endmember are normally distributed about the mean (Somers et al. 2011). Consequently, the technique has been frequently criticized owing to the predominantly non-normal distribution of endmember signatures, particularly in relation to vegetation (e.g. Zhang et al. 2006). An alternative method known as Multiple Endmember Spectral Mixture Analysis (MESMA) makes no such assumption as to the distribution of candidate endmember signatures (Roberts et al. 1998). MESMA is an iterative algorithm which models every possible LSU combination of intra-endmember variation and endmember quantity on a pixel-by-pixel basis (Dennison and Roberts 2003; Genú et al. 2013). Land cover abundance is consequently quantified using the LSU model combination with the best linear fit (i.e. the model with the lowest RMS error) on a per pixel basis (Roberts et al. 1998). Due to its ability to take into account the natural variation in endmember spectra, MESMA is currently the most widely used technique in spectral mixture analysis (Somers et al. 2011).

Materials and Methods

Study site

Kenfig Burrows is a stabilized dune system (650 ha) situated within Swansea Bay, South Wales, UK (CCW 2003). The dune field is a designated national nature reserve (NNR) (Fig. 1). The area is characterized by a net loss of sediment (Dargie 1995). Low sand availability for the propagation of pioneer species is affecting the biological diversity of the ecosystem, particularly towards the south of the dune system. Longshore drift has resulted in a more abundant sand supply in the north due to the redistribution of eroded sediment from the southern edge of the dune frontage (Dargie 1995). Concordantly, the mouth of the River Kenfig is the only known location of

early phase embryo dunes across the study area (Pye and Blott 2012).

Kenfig is of particular ecological value due to its shallow water table (Zhang and Baas 2012). This wet-dune regime causes saturated slack conditions with cyclical periods of subannual inundation, which is optimal for the development of pioneering hydrophytes (Avis 1992). Many of these early succession species are rare, for example, *Carex serotina* (green sedge), *Baldelia ranunculoides* (lesser water-plantain) and *Anagallis tenella* (bog pimpernel). Two cases in particular include the fen orchid (*Liparis loeselii*) and petalwort (*Petalophyllum ralfsii*) (Hurford 2006). At the European Union level, both these plants are listed as Annex II species (CCW 2003). As such, Kenfig is designated as a special area of conservation (SAC). The dune system supports an estimated 90–95% of the *L. loeselii* population within the UK (Lucas et al. 2002; BCBC 2008). Furthermore, the population at Kenfig is highly specialized. Leaf shape of the species at this location is uniquely rounded, as opposed to the commonplace elongated leaf structure leading to its subdivision as the variety: *L. loeselii* var. *ovata* (Pillon et al. 2007). Other rare pioneer species including sea dock (*Rumex rupestris*) and Welsh mudwort (*Limosella subulata*) are considered to be locally extinct due to the loss in sediment supply (BCBC 2002; Shanmugam et al. 2003). In its current stabilized state, the study area is dominated by creeping willow (*Salix repens*) as a mature slack species and fixed dune vegetation such as red fescue (*Festuca rubra*) and Lady's bedstraw (*Galium verum*) (BCBC 2008).

Datasets

A 73-year times series of change was created using Landsat archive imagery (30–60 m) from 1975 to 2014 (obtained from the USGS online data repository: https://earthexplorer.usgs.gov/) and aerial photography (1 m) [provided by the Royal Commission on the Ancient and Historical Monuments of Wales (RCAHMW)] from 1941 to 1962. The time series was used to predict BS abundance using: (1) brightness thresholding (aerial imagery) and (2) LSU (Landsat imagery) in comparison to observations made from concurrent high-resolution imagery. Specifically, an assessment of the effect of spatial resolution on abundance accuracy was carried out using WorldView 2 (2 m) imagery. Additionally an unmanned aerial vehicle (UAV) orthoimage (5 cm) was used to aid identification

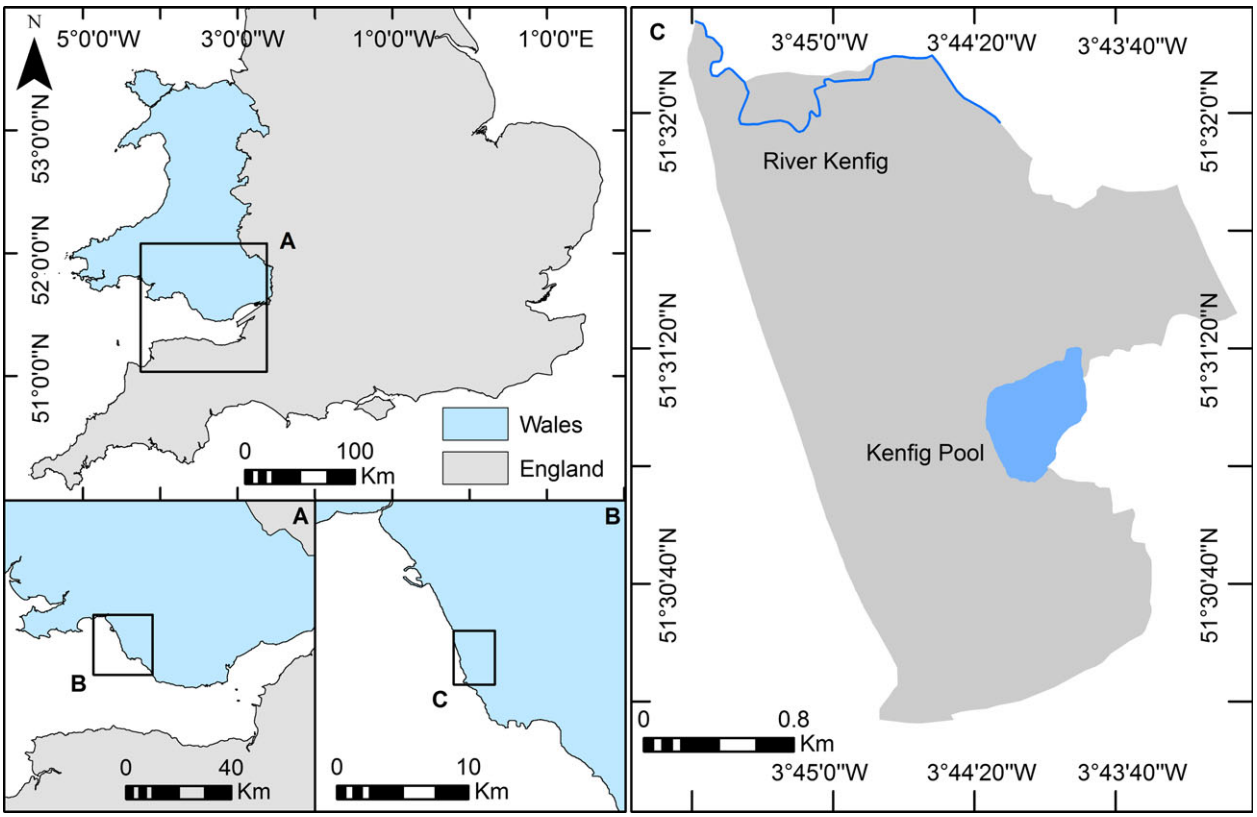

Figure 1. Location of Kenfig Burrows NNR, South Wales, UK.

of spectrally pure candidate pixel for unmixing of the WorldView 2 imagery, alongside field observations. Both high-resolution products were obtained from Natural Resources Wales (NRW). A complete overview of the imagery used within this investigation and acquisition dates can be found in Table 1.

All images were co-registered to the WGS84 UTM 30N projected coordinate system. The Landsat and WorldView imagery were orthorectified prior to the study and were corrected to at-surface reflectance using the 6SV atmospheric model implemented using the Python library ARCSI (Vermote et al. 1997; Wilson 2013).

Aerial imagery contained no predetermined geographical coordinates and required manual spatial adjustment. Georeferencing was performed in ArcMap 10.1 (Environmental Systems Research Institute, Redlands, CA, USA) using a second-order polynomial transformation. A 1:25 000 OS raster map (downloaded from the EDINA Digimap collection) formed the basemap for the transformation.

The orthorectified UAV image [generated using Structure from Motion using Agisoft Photoscan (Agisoft LLC, St. Petersburg, Russia)] was slightly misaligned with the WV2 image as the base-map product. Spatial error (Euclidean distance) was calculated in ArcMap 10.1 between the WV2 and UAV image using 40 sample points and a spatial correction was subsequently applied to the UAV image.

As the dune system covers a relatively small area (650 ha), Landsat image selection was limited to scenes with no observable cloud cover across study site. This resulted in a cross-seasonal acquisition range of April to September. Temporal frequency of the time series varied from interannual to decadal scale based on the limited availability of cloud-free scenes. Image compositing was used to infill areas of lost data due to the scan line corrector (SLC)-off mode for Landsat ETM+ images (2003–2012). Regions of missing data were substituted with pixels from an additional image, with a capture date as close as possible to that of the base image.

Image analysis

Endmember selection

Through repeated site visits during 2013 and reference to the UAV imagery, three candidate endmembers encompassing land cover within the study area were identified: green vegetation, BS and shade/moisture (S/M). The dual definition of the S/M endmember refers to the spectral properties of both water and shadow due to their spectral similarity following a similar approach adopted in other studies (Rashed et al. 2003). Pure pixel endmembers were identified and extracted from the data cloud of each image using the PPI (Effat et al. 2012) in ENVI 4.8. (Exelis Visual Information Solutions, Boulder, CO). A library of candidate spectral signatures associated with each image was subsequently generated for each endmember. The number of spectral bands between sensors differ: Landsat MSS (four bands), TM/ETM+ (six bands) and OLI (seven bands). This leads to slight differences in endmember spectra, and Figure 2 displays an example of the spectral properties for each of the three endmembers, derived from Landsat 8.

All WorldView endmember spectra were collected from within the study area itself by extracting candidate pure pixels from the data cloud and comparing their location to the UAV groundtruth image in ENVI 4.8. However, owing to the moderate spatial resolution of the Landsat

Table 1. List of remotely sensed datasets (LS = Landsat).

Type	Date	Spatial resolution (m)	Scene ID	Path/row
Aerial	22 October 1941	1		
Photography	9 June 1950	1		
	25 June 1962	1		
LS2 MSS	8 June 1975	60	LM22200241975159AAA05	220/24
LS5 MSS	16 August 1987	60	LM52040241987228AAA03	204/24
LS7 ETM+	3 September 1999	30	LE07_L1TP_203024_19990903_20170217_01_T1	203/24
LS7 ETM+	11 September 2002	30	EPP203R024_7F20020911	203/24
LS7 ETM+	22 June 2005	30	LE07_L1TP_204024_20050622_20170114_01_T1	204/24
LS5 TM	17 June 2006	30	LT05_L1TP_204024_20060617_20161121_01_T1	204/24
LS7 ETM+	1 June 2009	30	LE07_L1TP_204024_20090601_20161221_01_T1	204/24
LS5 TM	28 April 2011	30	LT05_L1TP_204024_20110428_20161208_01_T1	204/24
LS7 ETM+	27 July 2012	30	LE07_L1TP_204024_20120727_20161130_01_T1	204/24
LS8 OLI	16 August 2013	30	LC08_L1TP_203024_20130816_20170503_01_T1	203/24
LS8 OLI	15 May 2014	30	LC08_L1TP_203024_20140515_20170422_01_T1	203/24
WorldView2	22 July 2012	2		
UAV	July 2012	0.05		

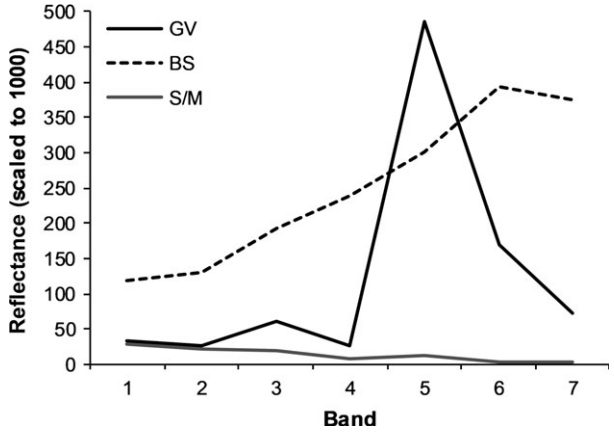

Figure 2. Example of endmember spectra derived from Landsat 8 (visible-IR spectral range: 0.43–2.29 μm across seven bands) for the three candidate endmembers: green vegetation (GV), bare sand (BS) and shade/moisture (S/M).

data, it was not possible to obtain pure pixels of BS and shade moisture from within the study site at Kenfig Burrows. Therefore, Landsat endmember regions were identified based on knowledge of the local area: S/M spectra were obtained from deep water pixels outside of Swansea Bay; BS spectra were obtained from the Pennant Standstone quarry 1 km south-east of the study area and in a region around the steel works in the Port Talbot Industrial Estate directly to the north (see Fig. 1). Both regions were considered to be a strong representation of BS spectra at Kenfig Burrows as they comprise of the same calcium-rich sand, derived from the Pennant Sandstone formation of South Wales (CCW 2003). Furthermore, while continuous BS cover was available within the study area, and also within proximal dune systems to the north, these regions were small and the abundance of pure pixels was negligible.

Multiple endmember spectral mixture analysis

Following selection and extraction of candidate endmember signatures spectral mixture analysis was undertaken using VIPER tools in ENVI 4.8. MESMA was applied to each Landsat image within the time series and to the 2012 WorldView2 product. In doing so, it was assumed that the reflectance signatures of each pixel were a linear sum of the reflectance of all subpixel components, weighted by abundance. The maximum possible number of endmembers that could be applied to any pixel was constrained to three to reduce the potential for collinearity and the subsequent over-fitting of the least-squares model (Chen et al. 2010; Canham et al. 2011) – a common issue in using data with low dimensionality such as multispectral satellite imagery.

Aerial photography analysis

Analysis of sand abundance within aerial photography (greyscale imagery) was made using density slicing of image brightness. Quantification of BS followed the methodology of (Pye and Blott 2011) where bright pixels synonymous with BS cover were discriminated and excluded from land cover (i.e. vegetation and water) with lower relative brightness. Brightness thresholds were derived through a manually iterative process by applying a density slicing function to each image in ENVI 4.8. The minimum BS threshold for each image ranged from a digital number value of 160–180. Thresholds were derived manually by comparing density slice boundaries to the extent of known sand deposits within each image.

Spatial resampling

To examine the relationship between abundance accuracy and spatial resolution, the 2 m WorldView2 dataset was resampled to 10-, 20-, 30-, 40- 50- and 60-m sized pixels using a pixel average aggregate function in ENVI 4.8. These images were subsequently unmixed. For ground-truth comparison to these coarse-resolution products, the original 2 m BS abundance image was rescaled accordingly, using the sum aggregate tool in Spatial Analyst Toolbox (ArcMap 10.1). Difference maps were subsequently created by subtracting the predicted abundance from actual abundance to identify the level of underestimation or overestimation per pixel. Difference across each map was then summed, and weighted average error ($\pm$ m^2 per pixel) identified.

Results

Change in BS cover 1941–2014

Overall, a trend of decreasing BS cover from 1941 to 2014 was identified for Kenfig Burrows (Fig. 3A and B). From 1941 to 1987, BS area decreased from 1.69 to 0.65 km^2, with a total loss of area of 1.04 km^2. From 1987 to 2002 change was limited within the range of 0.06 km^2. After 2002, fluctuations in BS area increased in range to 0.32 km^2 but showed an overall trend of decreasing area, when averaged at the decadal scale (averaged results from 2005 to 2014 saw an overall decrease to 0.51 km^2 compared to 0.72 km^2 in 2002, with a standard deviation of $\pm$0.12 km^2). The greatest drop within this period occurred between 2009 and 2011 with a loss of 0.32 km^2.

As illustrated in Figures 4 and 5, a clear decrease in BS cover occurred from 1975 to 1999 – this was particularly

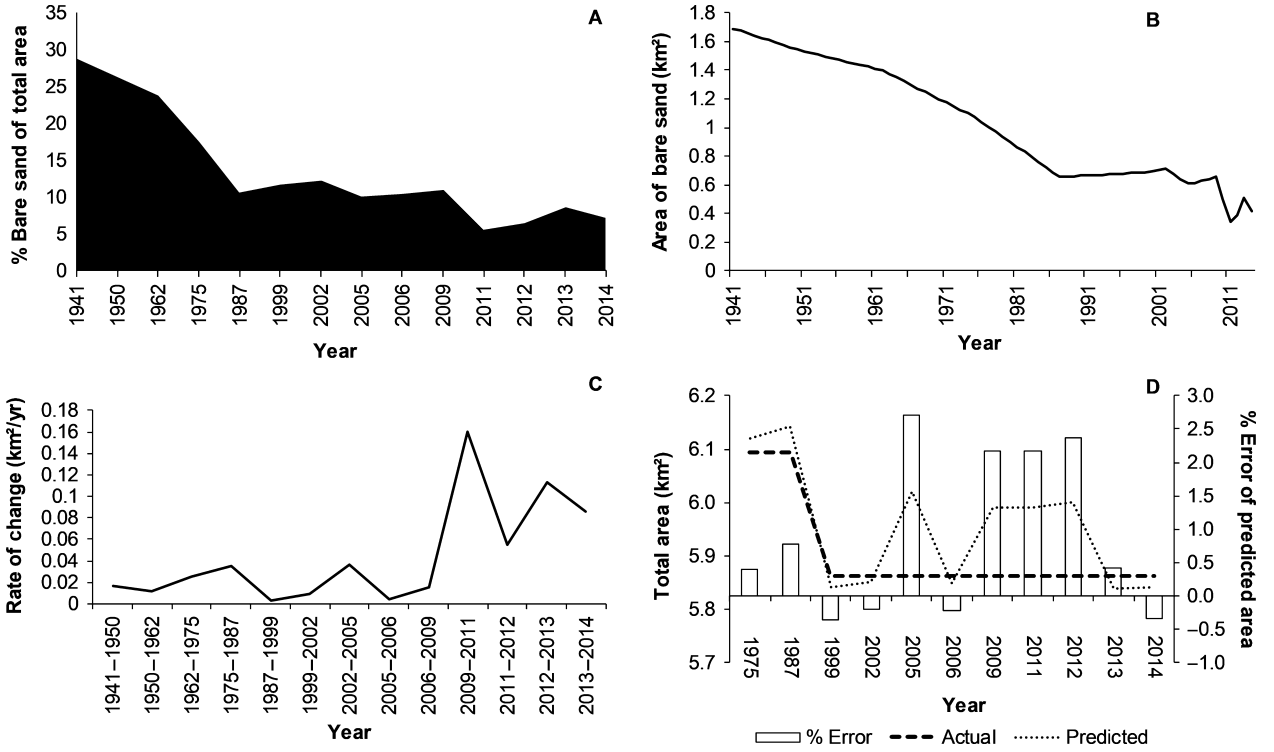

Figure 3. Analysis of historic change in the Kenfig Burrows dune system 1941–2014: (Aerial imagery 1941–1962; Landsat 1975–2014): (A) Extent of bare sand cover as a percentage of total area; (B) Area of bare sand (km^2); (C) Rate of change in bare sand cover (km^2/year); (D) Total area of study predicted by summed endmember abundance (km^2) versus actual area of study (km^2) with percentage error of area prediction.

noticeable in areas of continuous BS cover located in the north of the study area, coincidental with major land management interventions to stabilize the dune system. Between 1999 and 2011 changes continued to occur but were less pronounced with more subtle variations (with no particular trend of increase or decrease) in BS extent. The majority of change after 1999 was confined to fluctuations in the count of pixels with a sand coverage of <20% relative to the count of pixels of 20–40% (Fig. 6).

Rate of change in BS cover (Fig. 3C) remained consistent at <0.05 km^2/year between 1941 and 2009. After 2009, rate of change was more sporadic: 0.16 km^2/year (2009–2011), 0.06 km^2/year (2011–2012), 0.11 km^2/year (2012–2013) and 0.09 km^2/year (2013–2014), with an overall range of 0.11 km^2/year. This greater level of sporadicity was attributed to the higher temporal resolution of the time series after 1999, thereby allowing interannual fluctuations, often averaged-out at the decadal scale, to be quantified.

Accuracy assessment

Weighted average root-mean-square error (i.e. the difference between the original spectrum and the best-fit spectrum generated from unmixed endmember proportions) was calculated for each unmixed Landsat image between 1975 and 2014. All images were found to have an average RMS error of <10%.

Figure 3D displays error as predicted total area (i.e. summed abundance of all three endmembers in km^2) versus actual total area (km^2). Predicted total area for all unmixed images was always within 3% of actual area. Greatest percentage error was found for the years 2005, 2009, 2011 and 2012 at 2.71%, 2.18%, 2.18% and 2.37% respectively. This narrow increase in error for 2005, 2009 and 2012 was attributed to the composite nature of the imagery resulting from SLC failure of Landsat ETM+. Error increase for 2011 was attributed to age-related degradation of LS5 TM sensor (Markham et al. 2004). The sensor was decommissioned 7 months after acquisition of this image. Error was below 0.8% for all other years. This identified that the model adequately satisfied the unity constraint required for unmixing and proved that post-unmixing normalization was a suitable method for the removal of per pixel negativity.

Assessing the effect of spatial resolution

Total BS cover calculated from the 2012 WorldView image (2 m) was found to be 0.35 km^2 (Fig. 7). Weighted

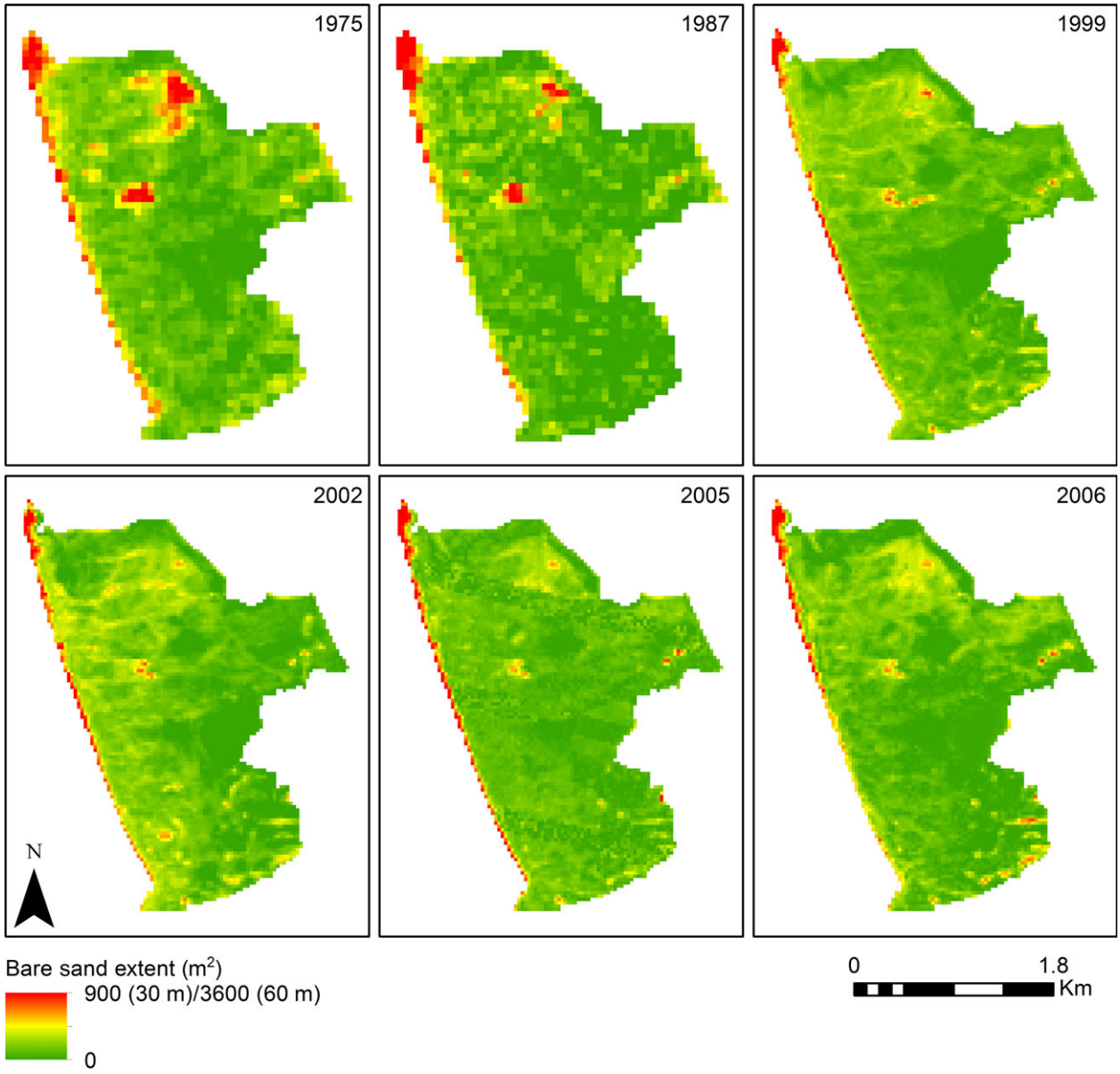

Figure 4. Landsat time series of change (1975–2006) of the Kenfig Burrows dune system.

average RMS error was calculated at 1.9%, with total predicted area of BS cover being under-estimated by 0.28%. Error in BS abundance was found to increase exponentially ($y = 2.59e^{0.0508x}$) with decreasing spatial resolution ($R^2 = 0.99$) (Fig. 8). Maximum error of ± 54.57 m^2 per pixel was identified at 60 m resolution.

When the exponential formula ($y = 2.59e^{0.0508x}$) derived from the resampled WV2 imagery was applied to the Landsat imagery, a spatial error margin of ± 54.49 m^2 per pixel was predicted for 60 m and ± 11.88 m^2 per pixel at 30 m. Taking all pixels into account, this resulted in a maximum error margin of $\pm 92\,197$ and $\pm 77\,351$ m^2, respectively, for 60 and 30 m images.

Unmixing of the 2012 WorldView image allowed a direct comparison with the Landsat estimate for the same year. A difference of 43 363 m^2 (12.39%) in BS estimation was identified between the two images (WV2 = 0.35 km^2; Landsat = 0.39 km^2). Taking into account only pixels that registered a proportion of BS >0 m^2, estimates for the 2012 Landsat image had a total spatial error margin of $\pm 71\,684$ m^2. The underestimation of area by the Landsat scene of 43 363 m^2 fell

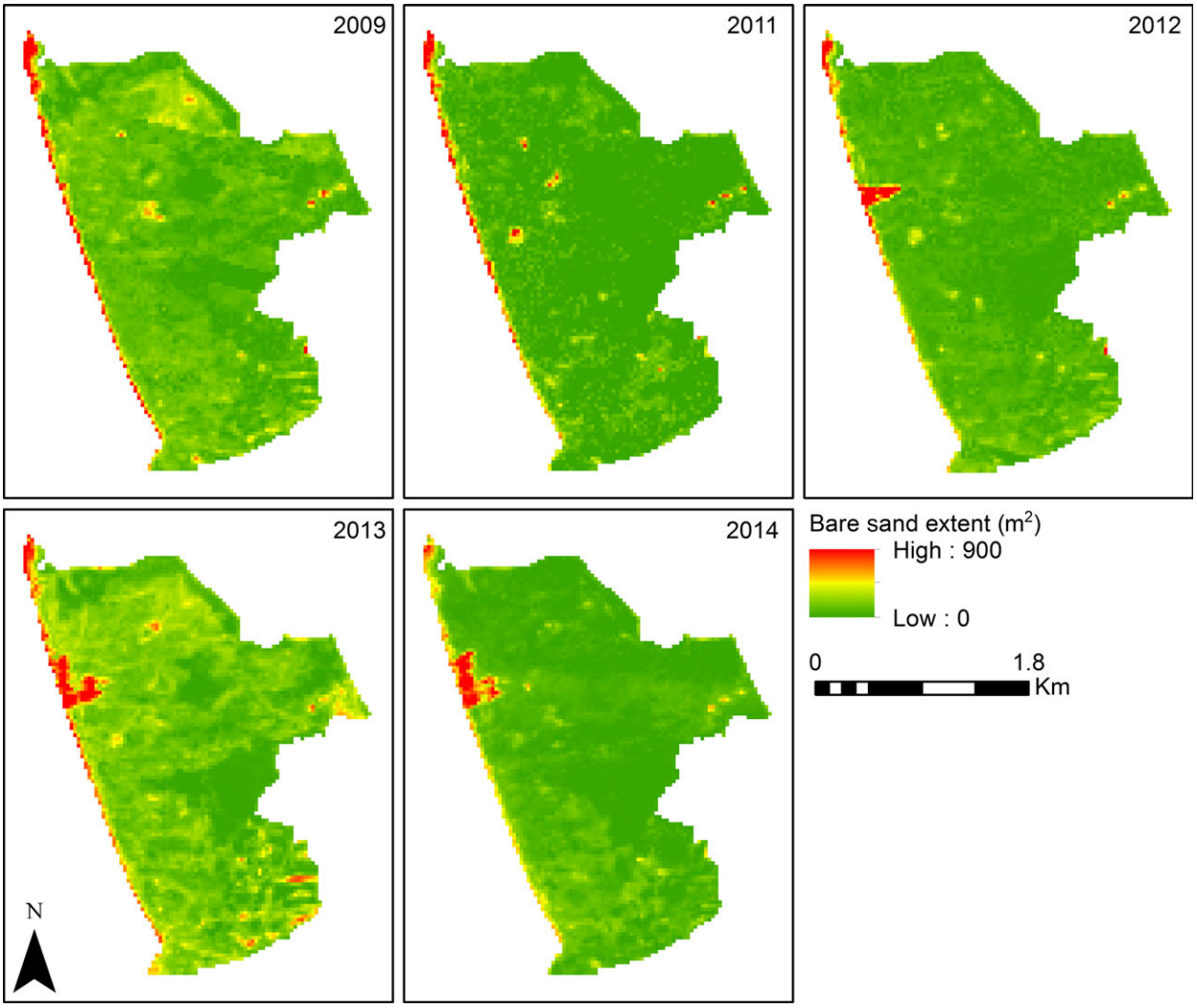

Figure 5. Landsat time series of change (2009–2014) of the Kenfig Burrows dune system.

comfortably within this margin of error. Therefore, any difference between BS estimation between the two images could be attributed to the reduced accuracy of the Landsat image in relation to its spatial resolution.

Interimage difference from 1999 to 2014 (i.e. all images with a spatial resolution of 30 m) was tested against the resolution-induced error margin to identify whether these variations were merely a product of the coarse resolution of the Landsat time series. Interimage difference in BS cover did not exceed the margin of error on four occasions (1999–2002, 2005–2006, 2006–2009 and 2011–2012) (Fig. 9). However, considering overall change within the cross-decadal period of 15 years (1999–2014) (0.378 km^2), difference did exceed spatial error limits. The change between coarser resolution images 1975 and 1987 (0.42 km^2) did exceed the spatial error margin at 60 m resolution. Therefore, sub-decadal difference in BS estimation exhibits a degree of error attributable to the spatial resolution limits of imagery at 30–60 m. However, authentic change at the inter-decadal scale was of a high enough magnitude to exceed variation as a result of resolution-based error.

Discussion

Results

This study presents a method for monitoring UK coastal dune habitats at a sub-Landsat pixel level that is appropriate for informing land cover managers for protecting and maintaining ecologically significant environments. Specifically, this study has successfully demonstrated how BS abundance can be tracked over time at the subpixel level as a proxy of ecological diversity. Accuracy metrics of the Landsat time series included RMS error and predicted total area versus

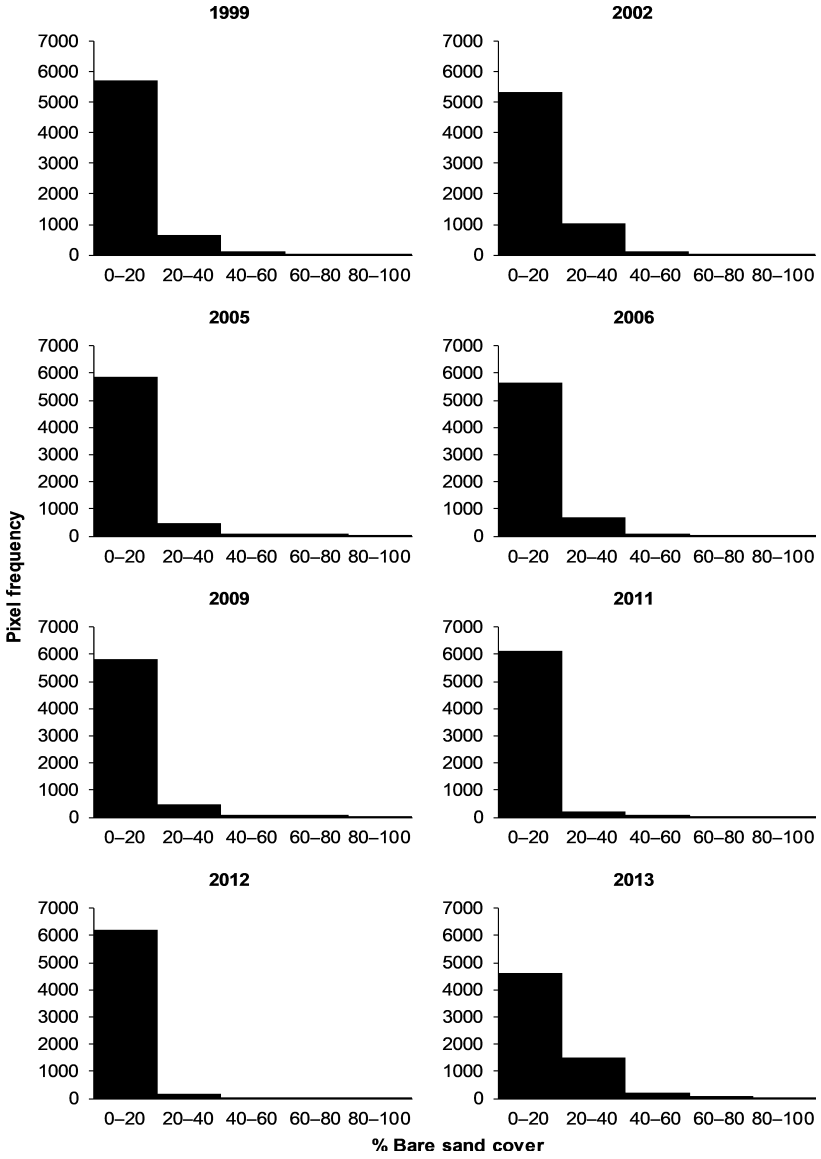

Figure 6. Sand abundance frequency distribution at the Kenfig Burrows dune system across Landsat time series (1999–2013).

actual total area. Both RMS error and area difference values were low across all images. This demonstrates the suitability of medium-resolution multispectral imagery at estimating BS cover using LSU. Coarse-resolution resampling of high-resolution data (2 m) showed that a decrease in resolution has an exponential effect on the accuracy of abundance estimation. Accordingly, the observed underestimation of BS extent by Landsat in comparison to WV2 (2012) could be explained entirely by resolution-induced spatial error. Similarly, in instances where interannual change in BS extent was negligible, actual change could not be separated from resolution-induced error.

Based on the analysis of the image time series, BS cover within the study site can be classified into two categories: (1) continuous BS – representing distinct large-scale features such as blowouts visible at 30 m spatial resolution; and (2) broad-scale BS – representing a general increase in BS availability across the study area, unconfined to distinct features. Figure 10 shows that Kenfig Burrows underwent rapid stabilization over a period of 73 years with an overall range of 1.36 km^2 in BS cover change. The majority of change took place between 1941 and 1987. Changes in cover were consistent with land use pressure and modification through biodiversity management.

In 1975, the majority of BS cover was confined to the upper reaches of the dune system in an area known as the Desert (Fig. 10). This area of sand was a remnant of

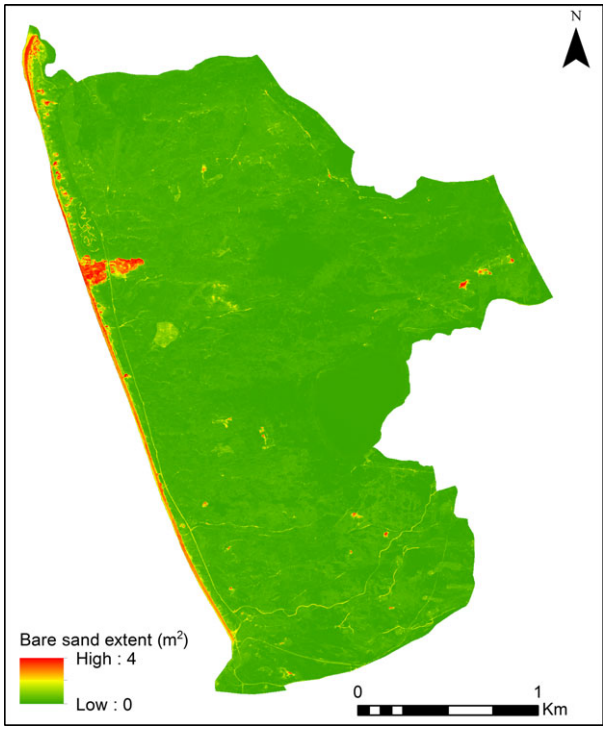

Figure 7. Bare sand abundance (2012) at the Kenfig Burrows dune system derived from WorldView 2 (2 m).

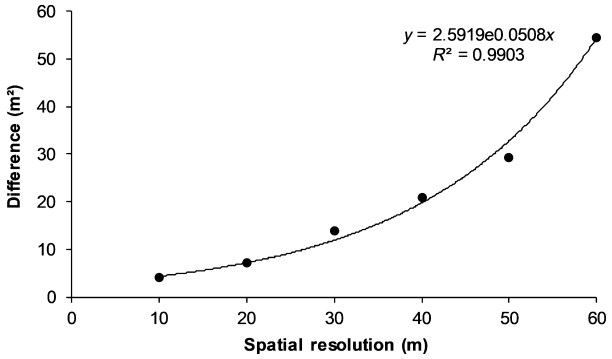

Figure 8. Relationship between spatial resolution and the mean difference per pixel between actual and predicted area of bare sand (m^2) for resampled WorldView 2 imagery, at the Kenfig Burrows dune system.

extensive land pressure during World War 2 when the dune system was used for military training purposes resulting in a extensive erosion. From 1975 to 2002, BS in this area reduced dramatically due to extensive stabilization works initiated during the 1960s. By 1999, this resulted in a small patch of continuous sand cover confined to the eastern corner of the Desert. This area persisted until 2009 but was subsequently lost by 2011. Despite a general trend in decreasing extent of BS cover,

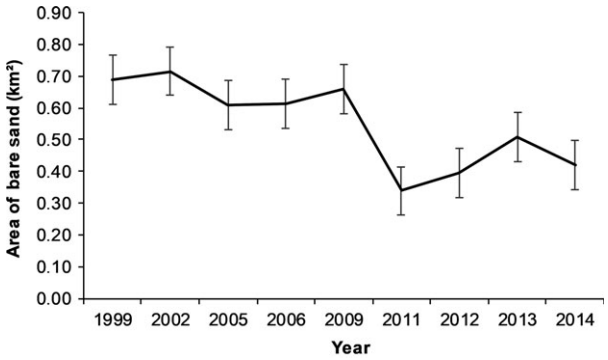

Figure 9. Change in bare sand extent 1999–2014 with error margins, defined by predicted level of resolution-derived error 30 m spatial resolution (see Figure 8), at the Kenfig Burrows dune system.

Figure 10 identifies the development of some new continuous BS features, such as the mown slack to the mid-west of the study site (2009 vs. 2011, Fig. 5). Furthermore, investigation of sand cover frequency distribution between 2009 and 2011 indicated a stabilization in areas with >40% sand cover and a reduction in areas with <20% BS (predominately vegetated areas). Additional new areas of BS include dune blowouts, freshly mown slacks and general areas of exposed sand created through visitor pressure (Fig. 10). One particular example of visitor pressure included three permanent areas of BS that can be seen within the north-eastern section of the dunes, north of Kenfig Pool. Another permanent area of sand exists in the south-west corner of the system (Fig. 10). The continued existence of this blowout was attributed to cattle activity, south of the dunes (Houston and Dargie 2010).

In some of the images (e.g. 2006, 2013 – Figs. 4 and 5), a moderate level of sand abundance can be observed within the south-east of the study site. This area is situated within the Pyle and Kenfig golf course (Fig. 10). Abundance within this section is most likely the result of associated activities such as close-mowing of the fairway and subsequent exposure of the sandy substrate beneath, alongside the obvious persistence of artificial sand bunkers. The presence of such activities coinciding with image acquisition may partially account for the 28.8% rise in sand abundance from 2012 to 2013. This is supported by an increase in pixels with >60% BS indicating the increased presence of continuous BS features.

Many changes in sand cover that can be observed within the time series are a product of biodiversity management efforts. Of particular note is the initiation of dune rejuvenation works which began during the winter of 2011/2012. This experimental development was focused on increasing sand delivery to the dune system interior through the eastward excavation of a BS corridor. Frontal dunes within this area were lowered and the excavated

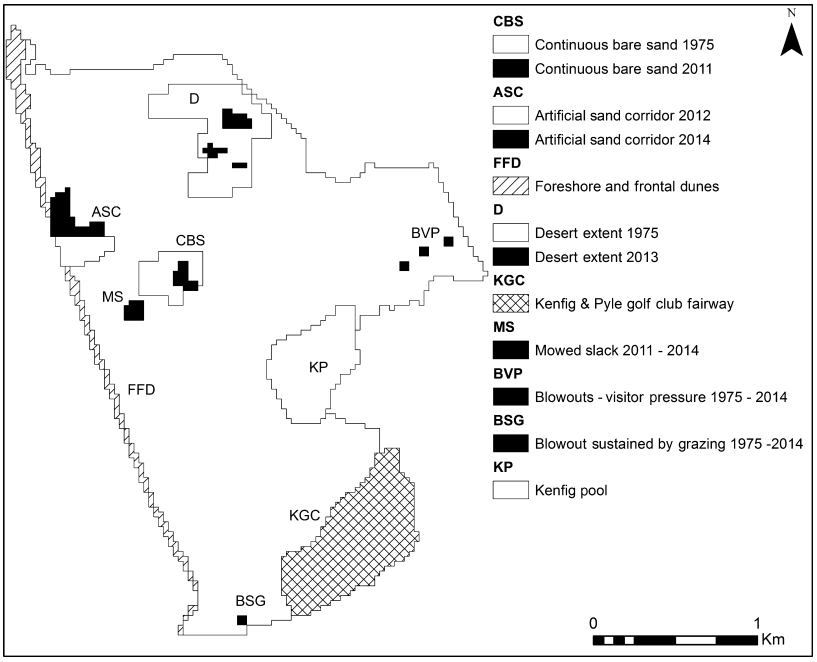

Figure 10. Thematic map of change in bare sand 1975–2014 derived from Landsat time series of bare sand abundance change at the Kenfig Burrows dune system.

sand relocated to the periphery of the corridor in order to increase wind funnelling. Phase 1 of the project was completed in 2012 and can be observed in the north-west of the study area in Figure 5. Phase 2 (the excavation of smaller corridors north of the Phase 1 zone) was completed in 2013 (Pye and Blott 2017), consistent with the rise in sand abundance from 2012 to 2013.

Management efforts have also been focused on directly encouraging the growth of rare hydrophytes such as *L. loeselii* through the close-mowing of dune slack areas (Rhind and Jones 1999). Although this practice does not create areas of continuous BS, cutting the sward short exposes the underlying sand and appears as areas of slightly greater abundance than the surrounding area. An example of this can be observed in Figure 10.

The rapid stabilization of Kenfig Burrows can also be attributed to the loss of grazing pressure during the 20th century. As with most UK coastal dune systems, grazing pressure at the site was historically high until the start of World War 2 and subsequently declined thereafter. Rabbit populations, also contributing to the persistence of short vegetative sward and increased sand mobility were also severely reduced following the 1954 myxomatosis outbreak. Rabbit numbers have never fully recovered (Pye and Blott 2017). In 2006, NRW (then CCW) attempted to mitigate the situation by enclosing 1.9 km^2 of the dune system with fencing to allow for controlled cattle grazing. However, to date, this increased grazing pressure has had little effect on the abundance of mobile sand in the study site (Pye et al. 2014).

Study limitations

The effects of spatial resolution were determined by spatially aggregating the 2 m Worldview imagery. In this instance, an average aggregate function was used but this does not explicitly model the point spread function (PSF) of the modelled sensor (Huang et al. 2002). It is suggested that a Gaussian PSF resampling method that weights the radiance reflected in relation to the centre of the IFOV (instantaneous field of view) might better reproduce the characteristics of a coarser resolution sensor (Bian and Butler 1999; Matheson and Dennison 2012). However, there is evidence to suggest that there is little difference between the two functions (Matheson and Dennison 2012), suggesting that average aggregation is a suitable representation of resolution-derived differences in pixel fractions.

Changes in BS over time can be estimated with a promising degree of accuracy by applying LSU as a sub-pixel technique to medium-resolution satellite imagery. This study consequently proposes the use of medium-resolution imagery, particularly with regards to the Landsat archive, for purposes of multiscale continuous monitoring of coastal dune systems. However, when considering the use of such data, it is important to take the following into

account: Estimates from medium-resolution imagery may include a low-to-moderate degree of operational-induced error. This study has identified that a decrease in spatial resolution has an associated decrease in the accuracy of BS estimates through the resampling of high-resolution data to coarse resolutions. However, a spatial margin of error can be identified based on this exponential relationship. Future studies should look towards refining the relationship between spatial resolution and abundance accuracy using actual data at multiple resolutions rather than modelling accuracy through the average aggregation of high-resolution data. Temporal resolution of the data is a significant factor in the representation of BS cover. Trends in coverage increase and decrease are observable at the decadal resolution. However, coverage has also been proven to fluctuate on a sub-decadal scale. At this scale, it is important to consider that image acquisitions are mere 'snapshots' in the representation of ecosystem health. As such, BS estimates may be sensitive to short-term conditions such as close-mowing activities in dune slacks or storm events which coincide with but do not accurately represent overall annual change. This may have been exacerbated to a degree by the low number of cloud-free scenes, enforcing a cross-seasonal time series, with image acquisition dates ranging from April to September (Table 1). Where possible, future study should look towards using seasonal or annual averages of BS cover using multiple images to reduce sensitivity to short-term change.

Future applications to biodiversity monitoring

When changes in BS cover are below a certain threshold, resolution-induced error can impact on the use of medium-resolution data for ecosystem health monitoring in dune systems. This study has presented a tractable method for error threshold quantification. Overall, monitoring of dune systems at 30–60 m resolution will be most applicable to monitoring large-scale changes, reflecting long-term, system-wide stabilization conditions. The approach used in this study is transferable to other dune systems helping to identify and mitigate for the effects of key drivers of long-term biodiversity loss such as climate change or land use change. Furthermore, this approach can be used for monitoring the effect of intervention measures including dune excavation (Pye and Blott 2017).

Multiple resolution testing has demonstrated that data sources such as Sentinel 2 MSI as a higher resolution alternative (10 m) to Landsat 8 OLI have the potential to improve the spatiotemporal constraints on continuous monitoring through spectral unmixing. In combination, Landsat 8 OLI and Sentinel 2A/2B have a global average revisit interval of 2.9 days (Li and Roy 2017). The improved temporal resolution will increase the potential for reliable sand abundance estimates to be made, calculated through multi-scene averaging, to remove noise from short-term change. Furthermore, it will enhance the monitoring of sand dune systems where long-term, high magnitude change is expected to occur more rapidly, in comparison to the historic changes observed at Kenfig. Landsat 8 OLI and Sentinel 2 MSI are also complementary in wavelength and geographic coordinate system, thereby allowing improvements to continuous monitoring through data fusion (Wang et al. 2017). However, the effect of data fusion techniques on the integrity of spectral mixture models is yet to be accounted for.

This study focuses on sand dune habitats, but the approach followed has potential for use in subpixel level monitoring across other dynamic ecosystems where large-scale change is resulting in habitat loss. Examples include the loss of water bodies for migratory bird species in ephemeral wetlands (Walther 2016) and the decline in seminatural grassland for red-listed birds in Boreal Agricultural-Forest Mosaics (Virkkala et al. 2004). Furthermore, the methods employed in this study could be replicated using open access resources such as Google Earth Engine, enabling land managers and non-remote sensing experts to apply the approach directly.

Conclusions

By using freely available satellite imagery alongside archived historical aerial photography, we present a potentially operational technique for monitoring coastal dune systems. This resulted in an assessment of BS cover change for Kenfig Burrows, South Wales (UK) over a 73 year period. The application of LSU as a subpixel technique allows changes in BS availability to be mapped, as a proxy of sand dune stabilization over time. However, time-series analysis using 30–60 m optical data is subject to a degree of resolution-dependent error that can affect the integrity of small-scale differences in BS extent. This study presents a robust method for estimating the degree of spatial error expected per pixel in the quantification of BS abundance. Results suggest that the spatiotemporal dynamics of large-scale changes within sand dune systems, consistent with dune stabilization or reactivation will exceed resolution-based error. However, medium-resolution data offers limited use in monitoring short-term and small-scale change such as seasonal or interannual shifts in sand distribution within stabilized systems. Overall, time-series analysis showed that major stabilization of Kenfig Burrows took place over the last 73 years in relation to land stabilization practices and a regional net loss in sediment supply. This has resulted in the loss of early successional species reliant on the colonization of BS regions.

Subsequent management strategies in recent years such as slack mowing and dune excavation have therefore focused on the remobilization of sand, resulting in an increase in sand availability. The availability of aerial photography over the study region allowed the length of the time series to be extended by 34 years beyond the advent of space-borne imagery. The temporal data range of other coastal dune systems may not be comparable in length. However, the Landsat archive alone provides over 40 years of historic coverage for the implementation of change detection across dune systems. Continuity of the Landsat mission and higher resolution systems [e.g. Sentinel 2 MSI (10 m)] ensures that continuous monitoring as part of an informed approach to sand dune management will remain viable on a long-term basis. The use of such methods has the potential to extend beyond sand dune management to other dynamic ecosystems, susceptible to large-scale changes in land cover and land use.

Acknowledgments

Georgina Ettritch's, MSc was funded by the European Social Fund (ESF) through the European Union's Convergence programme administered by the Welsh Government, with the support of Environment Systems Ltd as the industrial partner. All staff at Environment Systems Ltd are thanked for their support. WorldView 2 and UAV data were kindly provided by NRW. Clive Hurford at NRW is particularly thanked for making the purchase of the WorldView 2 imagery possible and supporting the wider project. Thanks also go to Derek Elliot at the Welsh Government and also to the Royal Commission on the Ancient and Historic Monuments of Wales (RCAHMW) for the provision of aerial photography.

Conflicts of Interest

The authors declare no conflict of interest. The founding sponsors had no role in the design of the study; in the collection, analyses, or interpretation of data; in the writing of the manuscript; and in the decision to publish the results.

References

Adams, J. B., M. O. Smith, and A. R. Gillespie. 1993. Imaging spectroscopy: interpretation based on spectral mixture analysis. Pp. 145–166 *in* C. M. Pieters and A. J. Englert, eds. *Remote geochemical analysis: elemental and mineralogical composition*, 1st ed. Cambridge University Press, Cambridge, UK. 9780521402811.

Adams, J. B., D. E. Sabol, V. Kapos, R. A. Filho, D. Roberts, M. O. Smith, et al. 1995. Classification of multispectral images based on fractions of endmembers: application to land-cover change in the Brazilian Amazon. *Remote Sens. Environ.* **52**, 137–154. https://doi.org/10.1016/0034-4257(94)00098-8

Ahmady-Birgani, H., K. G. McQueen, M. Moeinaddini, and H. Naseri. 2017. Sand dune encroachment and desertification processes of the Rigboland Sand Sea, Central Iran. *Sci. Rep.* **7**, 1523.

Asner, G. P. 1998. Biophysical and biochemical sources of variability in canopy reflectance. *Remote Sens. Environ.* **64**, 234–253. https://doi.org/10.1016/S0034-4257(98)00014-5

Asner, G. P., and D. B. Lobell. 2000. A biogeophysical approach for automated SWIR unmixing of soils and vegetation. *Remote Sens. Environ.* **74**, 99–112. https://doi.org/10.1016/S0034-4257(00)00126-7

Avis, A. M. 1992. Coastal dune ecology and management in the Eastern Cape. PhD Thesis, Rhodes University, South Africa.

Barducci, A., and A. Mecocci. 2005. Theoretical and experimental assessment of noise effects on least-squares spectral unmixing of hyperspectral images. *Opt. Eng.* **44**, 087008. https://doi.org/10.1117/1.2010107

BCBC. 2002. Local biodiversity action plan – volume 2: species and habitat action plans. Technical Report, Bridgend County Borough Council. Available at: https://www.bridgend.gov.uk/media/143793/Local_Biodiversity_Action_Plan___Volume_2__Habitat_and_Species_Action_Plans_.pdf. Accessed 1 July 2013.

BCBC. 2008. Habitats regulations assessment of the Bridgend local development plan – pre-deposit proposals. Technical Report, Bridgend County Borough Council. Available at: https://www.bridgend.gov.uk/media/148893/Pre_Deposit_Proposals4.pdf. Accessed 1 July 2013.

Bian, L., and R. Butler. 1999. Comparing effects of aggregation methods on statistical and spatial properties of simulated spatial data. *Photogramm. Eng. Remote Sensing* **65**, 73–84.

Canham, K., A. Schlamm, B. Basener, and D. Messinger. 2011. High spatial resolution hyperspectral spatially adaptive endmember selection and spectral unmixing. *in* S. Sylivia and P. E. Lewis, eds. SPIE 8048, Algorithms and Technologies for Multispectral, Hyperspectral, and Ultraspectral Imagery XVII, Proceedings of SPIE Defense, Security, and Sensing, Orlando, FL, USA, 29 June 2011.

CCW. 2003. Formal ecological summary of Kenfig NNR. Technical report, Countryside Council for Wales (CCW).

Chang, C. I. 2013. *Hyperspectral data processing: algorithm design and analysis*, 1st ed. Pp. 319–322. Wiley and Sons, Inc., NJ, USA. 9780471690566.

Chang, C. I., and D. C. Heinz. 2000. Constrained subpixel target detection for remotely sensed imagery. *IEEE Trans. Geosci. Remote Sens.* **38**, 1144–1159. https://doi.org/10.1109/36.843007

Chang, C. I., and A. Plaza. 2006. A fast iterative algorithm for implementation of pixel purity index. *IEEE Geosci. Remote*

Sens. Lett. **3**, 63–67. https://doi.org/10.1109/LGRS.2005.856701

Chen, X., J. Chen, X. Jia, and J. Wu. 2010. Impact of collinearity on linear and nonlinear spectral mixture analysis. Pp. 1–4 *in* Hyperspectral Image and Signal Processing: Evolution in Remote Sensing (WHISPERS), 2nd Workshop on, Reykjavik, Iceland, 14–16 June 2010, IEEE.

Clarke, M. L., and H. M. Rendell. 2009. The impact of North Atlantic storminess on western European coasts: a review. *Quat. Int.* **195**, 31–41. https://doi.org/10.1016/j.quaint.2008.02.007

Clarke, M. L., and H. M. Rendell. 2011. Atlantic storminess and historical sand drift in Western Europe: implications for future management of coastal dunes. *J. Coast. Conserv.* **15**, 227–236. https://doi.org/10.1007/s11852-010-0099-y

Dargie, T. C. D. 1995. *Sand dune survey of Great Britain, part 3 – Wales*, 1st ed. Pp. 1–155. Joint Nature Conservation Committee (JNCC), Peterborough.

Dennison, P. E., and D. Roberts. 2003. Endmember selection for multiple endmember spectral mixture analysis using endmember average RMSE. *Remote Sens. Environ.* **87**, 123–135. https://doi.org/10.1016/S0034-4257(03)00135-4

Drake, N. A., S. Mackin, and J. J. Settle. 1999. Mapping vegetation, soils, and geology in semiarid shrublands using spectral matching and mixture modeling of SWIR AVIRIS imagery. *Remote Sens. Environ.* **68**, 12–25. https://doi.org/10.1016/S0034-4257(98)00097-2

Effat, W., O. Hegazy, and M. NourEldien. 2012. Sub pixel classification analysis for hyperspectral data (Hyperion) for Cairo region, Egypt. *JEES* **2**, 80–89.

Genú, A. M., D. Roberts, and J. A. M. Demattê. 2013. The use of multiple endmember spectral mixture analysis (MESMA) for the mapping of soil attributes using ASTER imagery. *Acta Sci. Agron.* **35**, 377–386. https://doi.org/10.4025/actasciagron.v35i3.16119

Gong, P., and A. Zhang. 1999. Noise effect on linear spectral unmixing. *Geogr. Inf. Sci.* **5**, 52–57. https://doi.org/10.1080/10824009909480514

Heinz, D. C., and C. I. Chang. 2001. Fully constrained least squares linear spectral mixture analysis method for material quantification in hyperspectral imagery. *IEEE Trans. Geosci. Remote Sens.* **39**, 529–545. https://doi.org/10.1109/36.911111

Hoffman, M., S. Adam, L. Baert, D. Bonte, and N. Chavatte. 2005. Integrated monitoring of nature restoration along ecotones, the example of the Yser Estuary. *in* J. L. Herrier, A. Mees, A. Salman, J. Seys, H. Van Nieuwenhuyse and I. Dobbelaere, eds. International Conference on Nature Restoration Practices in European Coastal Habitats, Proceedings Dunes and Estuaries, Koksijde, Belgium, 19–23 September 2005.

Horwitz, H. M., R. F. Nalepka, P. D. Hyde, and J. P. Morgenstern. 1971. Estimating the proportions of objects within a single resolution element of a multispectral scanner. Pp. 1307–1320 *in* International Symposium on Remote Sensing of Environment, 7th, University of Michigan, Ann Arbor, Michigan, USA, 17–21 May 1971, Proceedings. Volume 2. (A72-11776 02-13), University of Michigan, Ann Arbor.

Houston, J. A., and T. C. D. Dargie. 2010. A study to assess stakeholder support for implementing a programme of dune re-mobilization on selected dune systems in Wales. CCW Contract Science Report No. 936., Technical Report, Countryside Council for Wales, Bangor.

Hu, Y. H., H. B. Lee, and F. L. Scarpace. 1999. Optimal linear spectral unmixing. *IEEE Trans. Geosci. Remote Sens.* **37**, 639–644. https://doi.org/10.1109/36.739139

Huang, C., J. R. G. Townshend, S. Liang, S. N. V. Kalluri, and R. S. DeFries. 2002. Impact of sensor's point spread function on land cover characterization: assessment and deconvolution. *Remote Sens. Environ.* **80**, 203–212. https://doi.org/10.1016/S0034-4257(01)00298-X

Hurford, C. 2006. Remote sensing of dune habitats at Kenfig NNR. Pp. 341–352 *in* C. Hurford and M. Schneider, eds. *Monitoring nature conservation in cultural habitats: a practical guide and case studies*, 1st ed. Springer Science and Business Media B.V., Dordrecht, The Netherlands. 9781402037573.

Jones, M. L. M., F. Hayes, S. A. Brittain, S. Haria, P. D. Williams, T. W. Ashenden, et al. 2002. Changing nutrient budget of sand dunes: consequences for nature conservation interest and dunes management: 2. Field survey. CCW Contract Science Report No. 566b. Technical Report, Centre for Ecology and Hydrology, Bangor.

Jones, M. L. M., H. L. Wallace, D. A. Norris, S. A. Brittain, S. Haria, R. E. Jones, et al. 2004. Changes in vegetation and soil characteristics in coastal sand dunes along a gradient of atmospheric nitrogen deposition. *Plant Biol. (Stuttg.)* **6**, 598–605. https://doi.org/10.1055/s-2004-821004

Karnieli, A. 1997. Development and implementation of spectral crust index over dune sands. *Int. J. Remote Sens.* **18**, 1207–1220. https://doi.org/10.1080/014311697218368

Kerdiles, H., and M. O. Grondona. 1995. NOAA-AVHRR NDVI decomposition and subpixel classification using linear mixing in the Argentinean Pampa. *Int. J. Remote Sens.* **16**, 1303–1325. https://doi.org/10.1080/01431169508954478

Levin, N., and E. Ben-Dor. 2004. Monitoring sand dune stabilization along the coastal dunes of Ashdod-Nizanim, Israel, 1945–1999. *J. Arid Environ.* **58**, 335–355. https://doi.org/10.1016/j.jaridenv.2003.08.007

Li, J., and D. P. Roy. 2017. A global analysis of Sentinel-2A, Sentinel-2B and Landsat-8 data revisit intervals and implications for terrestrial monitoring. *Remote Sens.* **9**, 902.

Lucas, N. S., S. Shanmugam, and M. Barnsley. 2002. Sub-pixel habitat mapping of a costal dune ecosystem. *Appl. Geogr.* **22**, 253–270. https://doi.org/10.1016/S0143-6228(02)00007-3

Markham, B. L., J. C. Storey, D. L. Williams, and J. R. Irons. 2004. Landsat sensor performance: history and current status. *IEEE Trans. Geosci. Remote Sens.* **42**, 2691–2694.

Matheson, D. S., and P. E. Dennison. 2012. Evaluating the effects of spatial resolution on hyperspectral fire detection and temperature retrieval. *Remote Sens. Environ.* **124**, 780–792. https://doi.org/10.1016/j.rse.2012.06.026

Pillon, Y., F. Qamaruz-Zaman, M. F. Fay, F. Hendoux, and Y. Piquot. 2007. Genetic diversity and ecological differentiation in the endangered fen orchid (*Liparis loeselii*). *Conserv. Genet.* **8**, 177–184. https://doi.org/10.1007/s10592-006-9160-7

Plassmann, K., M. L. M. Jones, and G. Edwards-Jones. 2010. Effects of long-term grazing management on sand dune vegetation of high conservation interest. *Appl. Veg. Sci.* **13**, 100–112. https://doi.org/10.1111/j.1654-109X.2009.01052.x

Potter, C., and J. Weigand. 2016. Analysis of desert sand dune migration patterns from Landsat image time series for the Southern California desert. *J. Remote Sens. GIS* **5**, 164. https://doi.org/10.4172/2469-4134.1000164

Provoost, S., M. L. M. Jones, and S. E. Edmondson. 2011. Changes in landscape and vegetation of coastal dunes in Northwest Europe: a review. *J. Coast. Conserv.* **15**, 207–226. https://doi.org/10.1007/s11852-009-0068-5

Pye, K., and S. J. Blott. 2011. Kenfig sand dunes – potential for dune reactivation. CCW Contract Science Report No. 971., Technical Report, Countryside Council for Wales (CCW). Available at: https://www.researchgate.net/publication/304146781_Kenfig_sand_dunes_Potential_for_Dune_Reactivation. Accessed 15 August 2013.

Pye, K., and S. J. Blott. 2017. Evolution of a sediment-starved, over-stabilised dunefield: Kenfig Burrows, South Wales, UK. *J. Coast. Conserv.* **21**, 685–717.

Pye, K., and S. J. Blott. 2012. A geomorphological survey of welsh dune systems to determine best methods of dune rejuvenation. CCW Contract Science Report No. 1002. Technical Report, Countryside Council for Wales (CCW). Available at: https://www.researchgate.net/publication/303965210_A_Geomorphological_Survey_of_Welsh_Dune_Systems_to_Determine_Best_methods_of_Dune_Rejuvenation. Accessed 15 August 2013.

Pye, K., S. Saye, and S. J. Blott. 2007. Sand dune processes and management for flood and coastal defence. Joint Defra/EA Flood and Coastal Erosion Risk Management R&D Programme, Technical Report, DEFRA. Available at: http://sciencesearch.defra.gov.uk/Document.aspx?Document=FD1302_5396_TRP.pdf. Accessed 15 August 2013.

Pye, K., S. J. Blott, and M. A. Howe. 2014. Coastal dune stabilization in Wales and requirements for rejuvenation. *J. Coast. Conserv.* **18**, 27–54. https://doi.org/10.1007/s11852-013-0294-8

Rajabi, R., and H. Ghassemian. 2013. Hyperspectral data unmixing using GNMF method and sparseness constraint. Pp. 1450–1453 *in* Geoscience and Remote Sensing Symposium (IGARSS) Proceedings, Melbourne, Australia, 21–26 July 2013, IEEE International.

Rashed, T., J. R. Weeks, D. Roberts, J. Rogan, and R. Powell. 2003. Measuring the physical composition of urban morphology using multiple endmember spectral mixture models. *Photogramm. Eng. Remote Sensing* **69**, 1011–1020.

Rhind, P., and P. S. Jones. 1999. The floristics and conservation status of sand-dune communities in Wales. *J. Coast. Conserv.* **5**, 31–42. https://doi.org/10.1007/BF02802737

Roberts, D., M. Gardner, R. Church, S. Ustin, G. Scheer, and R. O. Green. 1998. Mapping chaparral in the Santa Monica Mountains using multiple endmember spectral mixture models. *Remote Sens. Environ.* **65**, 267–279. https://doi.org/10.1016/S0034-4257(98)00037-6

Salih, A. A., E. T. Ganawa, and A. A. Elmahl. 2017. Spectral mixture analysis (SMA) and change vector analysis (CVA) methods for monitoring and mapping land degradation/desertification in arid and semiarid areas (Sudan), using Landsat imagery. *Egypt. J. Remote Sens. Space Sci.* **20**, S21–S29.

Saye, S. E., and K. Pye. 2007. Implications of sea level rise for coastal dune habitat conservation in Wales, UK. *J. Coast. Conserv.* **11**, 31–52. https://doi.org/10.1007/s11852-007-0004-5

Serrano, L., J. Penuelas, and S. L. Ustin. 2002. Remote sensing of nitrogen and lignin in Mediterranean vegetation from AVIRIS data: decomposing biochemical from structural signals. *Remote Sens. Environ.* **81**, 355–364. https://doi.org/10.1016/S0034-4257(02)00011-1

Shanmugam, S., and M. Barnsley. 1998. Linear spectral unmixing of CASI data for habitat mapping and management in a coastal dune system. Pp. 767–769 *in* T. I. Stein and K. Wilhelmson, eds. Geoscience and Remote Sensing Symposium (IGARSS) Proceedings, Seattle, USA, 6–10 July 1998, IEEE International (Vol. 2).

Shanmugam, S., N. Lucas, P. Phipps, A. Richards, and M. Barnsley. 2003. Assessment of remote sensing techniques for habitat mapping in coastal dune ecosystems. *J. Coast. Res.* **19**, 64–75.

Shumack, S., P. Hesse, and L. Turner. 2017. The impact of fire on sand dune stability: surface coverage and biomass recovery after fires on Western Australian coastal dune systems from 1988 to 2016. *Geomorphology* **299**, 39–53.

Silván-Cárdenas, J. L., and L. Wang. 2010. Fully constrained linear spectral unmixing: analytic solution using fuzzy sets. *IEEE Trans. Geosci. Remote Sens.* **48**, 3992–4002. https://doi.org/10.1109/TGRS.2010.2072931

Small, C. 2012. Spatiotemporal dimensionality and time-space characterization of multitemporal imagery. *Remote Sens. Environ.* **124**, 793–809. https://doi.org/10.1016/j.rse.2012.05.031

Smith, M. O., J. B. Adams, and D. E. Sabol. 1994. Spectral mixture analysis-new strategies for the analysis of multispectral data. Pp. 125–145 *in* J. Hill and J. Megier, eds. *Image spectroscopy a tool for environmental observations*, 1st

ed. Kluwer Academic Publishers, Dordrecht, The Netherlands. 0792329651.

Sohn, Y., and R. M. McCoy. 1997. Mapping desert shrub rangeland using spectral unmixing and modeling spectral mixtures with TM data. *Photogramm. Eng. Remote Sensing* **63**, 707–716.

Somers, B., S. Delalieux, J. Stuckens, W. W. Verstraeten, and P. Coppin. 2009. A weighted linear spectral mixture analysis approach to address endmember variability in agricultural production systems. *Int. J. Remote Sens.* **30**, 139–147. https://doi.org/10.1080/01431160802304625

Somers, B., G. P. Asner, L. Tits, and P. Coppin. 2011. Endmember variability in spectral mixture analysis: a review. *Remote Sens. Environ.* **115**, 1603–1616. https://doi.org/10.1016/j.rse.2011.03.003

Song, C. 2005. Spectral mixture analysis for subpixel vegetation fractions in the urban environment: how to incorporate endmember variability? *Remote Sens. Environ.* **95**, 248–263. https://doi.org/10.1016/j.rse.2005.01.002

Thackrah, G., P. Rhind, C. Hurford, and M. Barnsley. 2004. Using earth observation data from multiple sources to map rare habitats in a coastal conservation area. *J. Coast. Conserv.* **10**, 53–64. https://doi.org/10.1007/BF02818942

Tsoar, H. 2005. Sand dunes mobility and stability in relation to climate. *Physica A* **357**, 50–56. https://doi.org/10.1016/j.physa.2005.05.067

Tsoar, H., and J. T. Møller. 1986. The role of vegetation in the formation of linear sand dunes. Pp. 75–95 *in* W. G. Nickling, ed. *Aeolian geomorphology*, 1st ed. Allen and Unwin, London, UK. 0045511381.

Ustin, S. L., M. O. Smith, S. Jacquemoud, M. M. Verstrate, and Y. Govaerts. 1999. Geobotany: vegetation mapping for earth sciences. Pp. 189–249 *in* A. N. Rencz and R. A. Ryerson, eds. *Remote sensing for the earth sciences: manual of remote sensing*, 3rd ed. Volume 3. Wiley and Sons, Inc., NJ, USA. 9780471294054.

Van der Meer, F. D., and X. Jia. 2012. Collinearity and orthogonality of endmembers in linear spectral unmixing. *Int. J. Appl. Earth Obs. Geoinf.* **18**, 491–503. https://doi.org/10.1016/j.jag.2011.10.004

Vermote, E. F., D. Tanre, J. L. Deuze, M. Herman, and J. J. Morcette. 1997. Second simulation of the satellite signal in the solar spectrum, 6S: an overview. *IEEE Trans. Geosci. Remote Sens.* **35**, 675–686. https://doi.org/10.1109/36.581987

Virkkala, R., M. Luoto, and K. Rainio. 2004. Effects of landscape composition on farmland and red-listed birds in boreal agricultural-forest mosaics. *Ecography* **27**, 273–284.

Walther, B. A. 2016. A review of recent ecological changes in the Sahel, with particular reference to land-use change, plants, birds and mammals. *Afr. J. Ecol.* **54**, 268–280.

Wang, L., and X. Jia. 2009. Integration of soft and hard classifications using extended support vector machines. *IEEE Geosci. Remote Sens. Lett.* **6**, 543–547. https://doi.org/10.1109/LGRS.2009.2020924

Wang, Q., G. A. Blackburn, A. O. Onojeghuo, J. Dash, L. Zhou, Y. Zhang, et al. 2017. Fusion of Landsat 8 OLI and Sentinel-2 MSI data. *IEEE Trans. Geosci. Remote Sens.* **55**, 3885–3899.

Weng, Q., D. Lu, and J. Schubring. 2004. Estimation of land surface temperature – vegetation abundance relationship for urban heat island studies. *Remote Sens. Environ.* **89**, 467–483. https://doi.org/10.1016/j.rse.2003.11.005

Wilson, R. 2013. A python interface to the 6S radiative transfer model. *Comput. Geosci.* **51**, 166–171. https://doi.org/10.1016/j.cageo.2012.08.002

Zhang, L., and A. C. W. Baas. 2012. Mapping functional vegetation abundance in a coastal dune environment using a combination of LSMA and MLC: a case study at Kenfig NNR, Wales. *Int. J. Remote Sens.* **33**, 5043–5071. https://doi.org/10.1080/01431161.2012.657369

Zhang, J., B. Rivard, A. Sánchez-Azofeifa, and K. Castro-Esau. 2006. Intra-and inter-class spectral variability of tropical tree species at La Selva, Costa Rica: implications for species identification using HYDICE imagery. *Remote Sens. Environ.* **105**, 129–141. https://doi.org/10.1016/j.rse.2006.06.010

Zhang, C. L., Q. Li, Y. P. Shen, N. Zhou, X. S. Wang, J. Li, et al. 2018. Monitoring of aeolian desertification on the Qinghai-Tibet Plateau from the 1970s to 2015 using Landsat images. *Sci. Total Environ.* **619–620**, 1648–1659.

